

A Novel Approach to the Analysis of Altered Human Motor Synergistic Structures

Jingyao Chen[✉], Chen Wang[✉], Ningcun Xu[✉], Zeng-Guang Hou[✉] *Fellow, IEEE*, Liang Peng[✉],
Pingye Deng, Pu Zhang, and Chutian Zhang[✉]

Abstract—Motor synergy is considered as a motor control strategy deployed by the central nervous system (CNS), and it can be altered due to ageing, disease and injury. A timely assessment and analysis of altered motor synergy patterns will be helpful for the motor rehabilitation process. However, current research has mainly focused on the implementation of automated assessment scales. While the mechanism of the motor synergy structure alteration is not well understood yet. In this study, we proposed an approach to the analysis of altered human motor synergistic structures. By collecting and preprocessing the 3-dimensional motion data from 30 participants (including 15 stroke patients and 15 healthy individuals), synergistic structure features were extracted. We obtain the spatio-temporal vectors of motion by the non-negative matrix factorization. These vectors were clustered using K-means and matched with the scalar product. The similarity and specificity clustering pairs were obtained through Kuhn-Munkres Algorithm. The above results revealed that the structure of human motor synergy was greatly altered after stroke, and some new synergistic patterns with commonalities emerged during patients' movements. This study presents a new method to identify specific patterns of motor synergy arising

from disease-altered biomechanics and central nervous system, providing new targeted protocols for rehabilitation assessment.

Index Terms—Motor synergy structure, Motor variability, Neurorehabilitation, Nonnegative matrix factorization, K-means, Kuhn-Munkres algorithm.

I. INTRODUCTION

Human locomotion can be considered as the combination of a complex series of motor synergistic structural units. It can coordinate multiple causal variables (e.g., individual motor unit activation) into task-specific functional groups toward the goal of stabilizing the effects on dominant performance variables (e.g., completion of a specific motor task) [1]. Because of ageing [2], [3], cardiovascular diseases [4], [5], neurological diseases [6], and sports injuries [7], the human motor synergistic structure can be altered. Neuroplasticity is an important theoretical basis for motor rehabilitation, which means that the damaged parts of the nerve center will be reinvented by functional compensation. Clinical studies have shown that early rehabilitation can largely improve the motor function exploiting neural plasticity in the critical periods [8], [9], and quantitative assessments of motor disabilities play an important role in this process [10], [11].

The traditional approach to rehabilitation evaluation is to measure the patient's performance on assessment scales, such as the Fugl-Meyer Assessment [12] and the Berg Balance Scale, BBS [13]. Current research has focused on how to automate this process, with some studies using wearable devices to make the measurement process more convenient [14], [15]. The validity and reliability of these methods have been verified. However, these approaches often focus on scoring, and the mechanism of alteration of the motor synergy structure remains unclear.

Therefore, we hope to analyze the altered motor synergistic structure between patients with motor dysfunction and healthy participants from a kinematic perspective, which could provide more suggestions for the rehabilitation process. Thirty participants (including 15 stroke patients and 15 healthy subjects) from the Chinese Rehabilitation Research Center, Macau University of Science and Technology and the Institute of Automation, were recruited into the experiment. The upper and lower limb movement paradigms were completed under the guidance of rehabilitation physicians. After capturing and analyzing their 3D spatiotemporal movement data, we used the motor synergistic score to extract the synergistic structure features of the participants. By clustering

This work was supported in part by the National Key Research and Development Program of China under Grant 2022YFC3601200; in part by the National Natural Science Foundation of China under Grants U1913601, U21A20479 and 62203441; and in part by the Beijing Natural Science Foundation under Grant Z170003. (Corresponding author: Chen Wang; Zeng-Guang Hou.)

This work involved human subjects or animals in its research. Approval of all ethical and experimental procedures and protocols was granted by the Ethics Committee of China Rehabilitation Research Center.

Jingyao Chen is with the Faculty of Innovation Engineering, CASIA-MUST Joint Laboratory of Intelligence Science and Technology, Macau University of Science and Technology, Macao 999078, China, and also with the Institute of Analysis and Testing, Beijing Academy of Science and Technology, Beijing 100089, China (e-mail: 2009853pmi30003@student.must.edu.mo).

Chen Wang and Liang Peng are with the State Key Laboratory of Multimodal Artificial Intelligence Systems, Institute of Automation, Chinese Academy of Sciences, Beijing 100190, China (e-mail: wangchen2016@ia.ac.cn; liang.peng@ia.ac.cn).

Zeng-Guang Hou is with the State Key Laboratory of Multimodal Artificial Intelligence Systems, Institute of Automation, Chinese Academy of Sciences, Beijing 100190, China, and also with the School of Artificial Intelligence, University of Chinese Academy of Sciences, Beijing 100049, China (e-mail: zengguang.hou@ia.ac.cn).

Ningcun Xu and Chutian Zhang are with the Faculty of Innovation Engineering, CASIA-MUST Joint Laboratory of Intelligence Science and Technology, Macau University of Science and Technology, Macao 999078, China (e-mail: 2202853nmi30001@student.must.edu.mo; 2109853nmi30001@student.must.edu.mo).

Pingye Deng is with the Institute of Analysis and Testing, Beijing Academy of Science and Technology, Beijing 100089, China (e-mail: dengpingye@bpcpa.ac.cn).

Pu Zhang is with the Faculty of Innovation Engineering, CASIA-MUST Joint Laboratory of Intelligence Science and Technology, Macau University of Science and Technology, Macao 999078, China, and also with the Department of Rehabilitation Evaluation, China Rehabilitation Research Center, Beijing 100068, China (e-mail: 2009853pmi30002@student.must.edu.mo).

and analyzing the spatio-temporal features of movements, we found that human motor synergistic structures were greatly altered after stroke, and some synergistic structures with common features emerged in the patients' upper and lower extremities.

The rest of the paper is organized as follows. *Section II* describes the related work, *Section III* describes our approach, *Section IV* describes the experiments and results, and *Section V* gives the conclusions of the paper and discusses future directions for improvement.

II. RELATED WORK

Recently, related studies on movement patterns have focused on inter-muscular synergy through physiological signals, such as electromyography (EMG) signals. Many previous works have demonstrated that muscle synergies and clinical observation convey the same information on motor impairment [16], [17]. Such as Vincent C. K. Cheung. et al. [18] revealed how locomotor synergies change in training by studying the EMG and plantar pressure data during running in different populations. In our past studies, we assessed the patient's motion using a multimodal fusion algorithm by acquiring the participant's surface electromyography (sEMG) data [19], and used sEMG signals from participants to assess motor function by comparing the cosine similarity of synergistic modules [20].

All of the above studies have attempted to reveal the link between motor synergy and the neurocentral system through muscle, thus we hope to remove the intermediate medium and directly analyze the altered movement patterns between patients and healthy participants from a kinematic perspective, so as to provide more profound suggestions for the rehabilitation process.

III. METHODOLOGY

A. Posture Tracking Method

We used a vision-based human motion tracking method to reveal the synergistic patterns between key points of the human body during movement. Based on this method, the human body is labeled with 10 key points corresponding to the major joints required for daily activities, including the left shoulder (LS), right shoulder (RS), left elbow (LE), right elbow (RE), left knee (LK), right knee (RK), left ankle (LA) and right ankle (RA), as shown in Fig.1 a). By photographing the participants' limb movement paradigms (as shown in Fig.1 b)), the 3-dimensional trajectories during movement were extracted using the Mediapipe toolkit, as shown in Fig.1 c).

B. Motor Synergistic Score

In order to extract information about the participants' motor synergistic structures, we proposed a method for calculating the key joints' synergistic structure scores, as follows.

The displacement function of the i th joint position eigenvalue between the m th frame and the n th frame is defined as:

$$D(m, n, i) = \sqrt{(Jx_{m,i} - Jx_{n,i})^2 + (Jy_{m,i} - Jy_{n,i})^2 + (Jz_{m,i} - Jz_{n,i})^2} \quad (1)$$

where, $Jx_{m,i}$, $Jx_{n,i}$, $Jy_{m,i}$, $Jy_{n,i}$, $Jz_{m,i}$, $Jz_{n,i}$ are the coordinates of the i th eigenvalue at the m th and n th frames, respectively.

A value of energy for the i th joint motion in p th frame is defined as:

$$Energy(p, i) = D(p, p - 1, i) \quad (2)$$

Therefore, the energy of the expected motion joint in the p th frame can be represented as:

$$Locomotor_energy(p, L) = \frac{\sum_{i \in L} Energy(i)}{N_Locomotor} \quad (3)$$

where, the set L is determined by the motion task, which represents the index of joint features for the expected motion. For example, in the upper limb task paradigm (see Figure 1 b)), the set L includes joints RS, RE, and RW. $N_Locomotor$ represents the number of expected joint features required for that motion task.

Define the energy value of the connected motion joints in p th frame as:

$$Synergistic_energy(p, S) = \frac{\sum_{i \in S} Energy(i)}{N_Synergistic} \quad (4)$$

where, the set S is determined by the motion task, which represents the index of joint features for the collateral motion. For example, in the upper limb task paradigm (see Figure 1 b)), the set S includes joints LS, LE, LW, RK, LK, RA, and LA. $N_Synergistic$ represents the number of collateral joint features in the motion task.

From Eq(3) and Eq(4), we get the synergistic score in p th frame:

$$Synergistic_score(p, L, S) = \frac{Synergistic_energy(p, S)}{Locomotor_energy(p, L)} \quad (5)$$

We tried to characterize the difference in motion patterns by the variation of the synergy structure, so we extracted the synergy score of each frame as a feature for the next analysis.

C. Spatial-temporal Factorization Method

We deconstructed the synergetic data using the conventional spatial-temporal combination that interprets the multi-joints human motion as the product of the spatial matrix W and the temporal matrix T as follows:

$$M = WT \quad (6)$$

Many researches have shown that using the non-negative matrix factorization (NMF) method [17]–[20], the spatio-temporal pattern of motor joint synergy can be calculated, where the contribution of the joint synergy to the movement can be represented by the weight W and the activation time of the joint can be represented by a curve. As can be seen

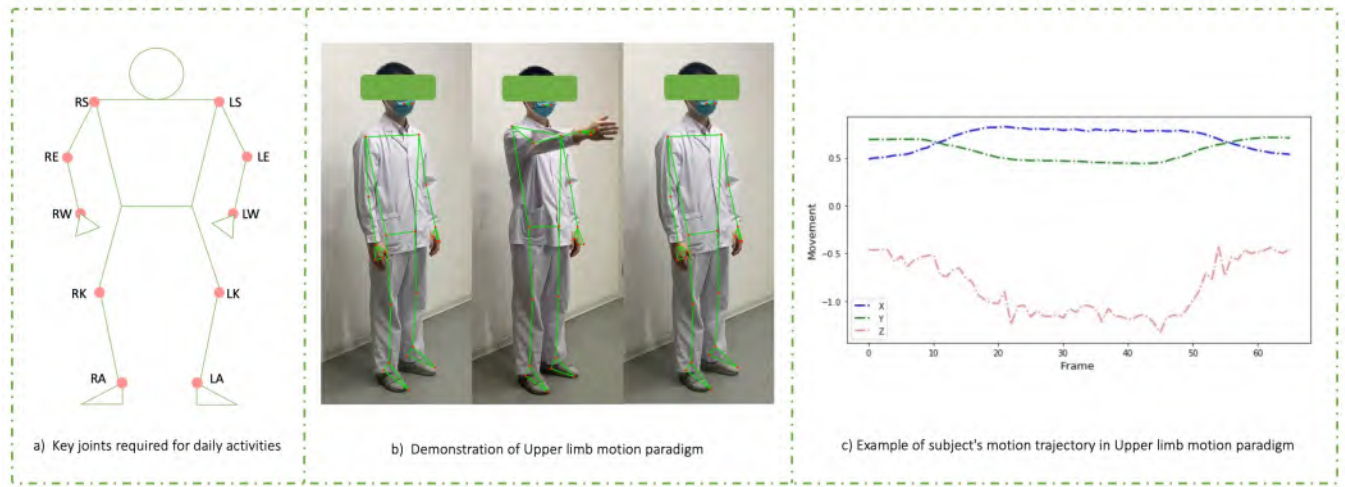


Fig. 1. Human key joints model & trajectory illustration. a) shows the 10 major joints required for daily activities. b) is the standard paradigm for upper limb tasks demonstrated by the rehabilitation physician. c) shows an example of the participant's motion trajectory in the upper limb tasks.

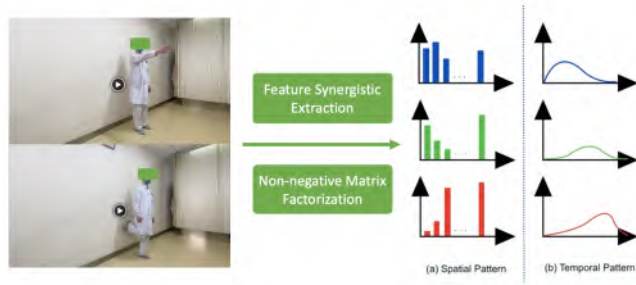


Fig. 2. Flow chart of spatio-temporal decomposition of synergistic features

in Fig.2. To determine the patterns of motor synergy, we extracted 10 synergy vectors, for each NMF implementation, the update rule is terminated when the inter-iteration variation between the reconstructed matrix and the original data is $<0.01\%$ in 200 consecutive iterations.

D. Representative Motor Synergy Vector Extraction Method

We determine the representative motor synergy vectors of different populations by the k-means clustering algorithm. According to this algorithm, we randomly selected k vectors from the sample set as cluster centers, then calculated the Euclidean distance between all samples and these k cluster centers. For each sample, it is assigned to the cluster with the closest cluster center. For each new cluster, a new cluster center is calculated. 300 iterations are performed with different random initial values, from which the cluster with the minimum point-to-centroid sum is selected.

Silhouette analysis can be used as a measure to indicate how closely samples are grouped in clusters [21]. Therefore, we used it to determine the number of synergistic clusters (i.e., the number of k) in each subjects group.

Firstly, we calculate the cluster cohesion, which is the average distance between a sample and all other points in

the same cluster:

$$Coh(i, C) = \frac{\sum_{i \in C, j \in C} Euclidean_distance(i, j)}{n - 1} \quad (7)$$

where the set C represents the set of samples in a certain cluster, n represents the number of samples in the set C , and $i, j \in C$. $Euclidean_distance(i, j)$ represents the Euclidean distance between samples i and j . The smaller the value of cluster cohesion, the more compact the class.

Then, we calculate the cluster separation from the next closest cluster as the average distance between the sample and all samples in the nearest cluster:

$$Spa(i, C, S) = \frac{\sum_{i \in C, j \in S} Euclidean_distance(i, j)}{ns} \quad (8)$$

where, the set C and the set S represent different clusters, ns represents the number of samples in the set S , and $j \in S, i \in C$. The calculation of $Spa(i, C, S)$ is similar to that of $Coh(i, C)$.

By traversing the other clusters to obtain multiple values and selecting the smallest value as the final result, we obtain:

$$Spa(i) = Min_{C \in M, S \in M} \{Spa(i, C, S_k)\} \quad (9)$$

where the set M is the set of all samples of the k clusters. The silhouette score can be defined as:

$$S(i) = \begin{cases} 1 - \frac{Coh(i, C)}{Spa(i)}, & Coh(i, C) < Spa(i) \\ 0, & Coh(i, C) = Spa(i) \\ \frac{Spa(i)}{Coh(i, C)} - 1, & Coh(i, C) > Spa(i) \end{cases} \quad (10)$$

We traverse the K values from 2-10, cluster under each K value, and calculate the silhouette coefficients Sum_S as:

$$Sum_S = \frac{\sum_{i \in M} S(i)}{nk} \quad (11)$$

where nk represents the number of samples in the set M . The most appropriate K -value for each population was selected by combining the silhouette coefficients and the elbow method.

E. Motor Synergy Similarity

We normalized the clustering centroid vectors of the extracted synergy clusters and compared the similarity of synergy between the two groups of participants by using its scalar product. We choose to categorize the synergistic vectors with scalar product >0.99 as matches. And using the Kuhn-Munkres algorithm to filter the most matched synergy vector pairs in the two groups of participants.

F. Motor Synergy Variability

Synergistic groups that do not pass the similarity screen will represent the altered motor synergy structures between the two groups of participants. We screened the specificized vectors of both participant groups and labeled the three key joints with the highest weight in this synergistic vector. By superimposing the heat maps, significant structural changes in motor synergy between healthy participants and patients can be found.

IV. EXPERIMENTS & RESULTS

A. Experimental Procedure

In this study, we recruited 15 stroke patients and 15 age-matched healthy participants in collaboration with the Chinese Rehabilitation Research Center and the Macau University of Science and Technology. Table I describes the demographic information of the 30 participants, including 15 in the Stroke Patients group (SP) and 15 in the Healthy Participant group (HP). We deliberately selected some relatively young participants to reduce changes in movement patterns due to ageing. The inclusion criteria for the post-stroke patients were: 1) the participant had been diagnosed with an ischemic or hemorrhagic stroke; 2) the participant had not been diagnosed with a cognitive dysfunction category; 3) the participant had no major post-stroke complications; and 4) participants were assessed by experienced therapists on the Fugl-Meyer scale with a score of 0 or 1 on both tasks. The inclusion criteria for the control group had no motor or neurological impairment.

This study was approved by the Ethics Committee of the China Rehabilitation Research Center. Before inclusion in the study, each participant was informed of the details and purpose of the experiment, and all signed a written informed consent form.

TABLE I
PARTICIPANTS DEMOGRAPHICS

	Post-stroke patients		Healthy participants	
	Males	Females	Males	Females
Numbers	8	7	9	6
Age(yrs)	41.3±17.1	39.5±13.6	37.3±9.4	40.3±11.5
S-F-UT	0(3)/1(5)	0(4)/1(3)	-	-
S-F-LT	0(5)/1(3)	0(4)/1(3)	-	-

* S-F-UT=Statistics on the number of patients scoring 0 and 1 in upper limb task, S-F-LT=Statistics on the number of patients scoring 0 and 1 in lower limb task.

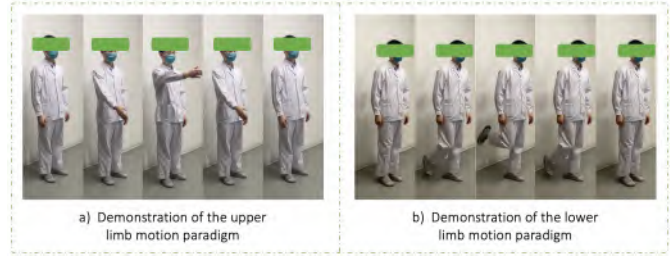


Fig. 3. Demonstration of the upper and lower limb motion paradigm

Guided by experienced rehabilitation physicians, we designed the motion paradigm, including the upper limb task and the lower limb task, as shown in Fig.3.

Upper limb task: Abduction of the shoulder 0-90° to the front.

Lower limb task: Flexion of the knee to 90° and the hip at 0°.

The participants completed the above two paradigms with video guidance, the video recording format was 1080p HD/30 fps.

B. Impact of Stroke on the Synergy Scores

Our 30x2 segments of motion 3-dimensional data for both participants groups were unified to 100 frames by padding and sampling. Then the synergy scores of 10 key joints of each frame were extracted, and four sets of 100x10 synergistic data were formed according to the participants' groups and movement paradigms. To ensure the uniformity of the data, the samples with the affected side as the left limb were mirrored. We summed and averaged the synergy

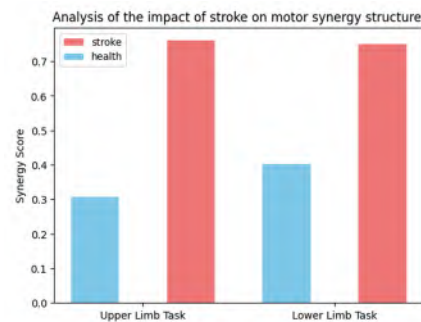


Fig. 4. Sequential symmetric convolution normalization flowchart

scores for each frame of the two groups to obtain the average synergy score. As shown in Fig.4, the synergy scores of stroke patients were higher than those of healthy participants in all tasks. This means that in order to complete the motor task, the patients mobilized more of the other joints to assist the primary joint or maintain balance.

C. Impact of Stroke on the Spatio-temporal Properties of Synergistic Structures

To further understand at which phase of the motion the joint contributes, we analyzed the spatio-temporal character-

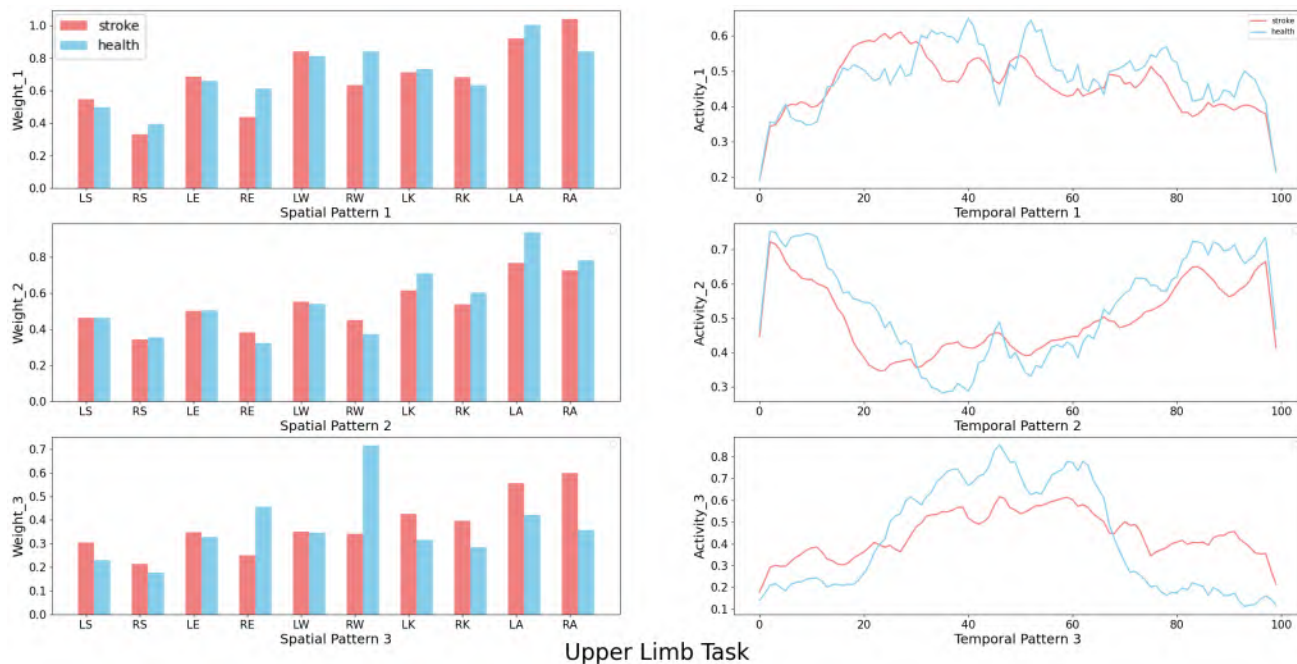


Fig. 5. The spatio-temporal patterns of the upper limb task

istics of the synergy using a non-negative matrix decomposition.

Fig.5 shows the three main spatio-temporal patterns of the upper limb task. In Spatial Pattern 1 we can see that the patients had higher activation on the contralateral upper limb (including joints LS, LE, and LW) than healthy participants. Spatial Pattern 2 and Temporal Pattern 2 show that the healthy participants had more lower limb joint oscillations than the patients during the initial and end phases of the motion, implying that patients pay more attention to the center of gravity and are more careful when doing upper limb movement.

Fig.6 shows the three main spatial-temporal patterns of the lower limb task. In Spatial Pattern 1 we can observe that the patients had higher activation on the contralateral upper and lower limbs (including joints LS, LE, LW, LK, and LA) than healthy participants. Spatial Pattern 2 and Temporal Pattern 2 show that the healthy participants had more ipsilateral upper limb joint oscillations than the patients during the initial and end phases of the motion. This implies that there is a significant difference in the movement pattern of the contralateral upper limb between patients and healthy participants during the unilateral standing task.

D. Disease-related Changes in Synergistic Structures

After the spatial-temporal decomposition, we traversed K values from 2 to 10. By combining the silhouette coefficients and the elbow method, we selected the K values for the SP and HP groups in the upper and lower limb tasks.

In the upper limb movement, we normalized the 9 clustering center vectors in SP and 8 clustering center vectors in HP and calculated the scalar products individually as weights. Using the Kuhn-Munkres Algorithm to solve the optimal

matching problem with weights, we selected the matched structures in two groups of synergies. The unmatched clustering centers were considered as the difference between the two groups of synergistic patterns.

In the upper limb task, the expected motor joints are the joints RS, RE, and RW. As shown in Fig.7, there are 4 matched synergistic structures between the healthy participants and the patients. Significant involvement of the contralateral ankle (LA) and ipsilateral knee (RK) joints can be observed during the task, so we hypothesized that both lower limbs need to maintain balance by swaying their center of gravity during upper limb movements.

As shown in the specific vector pairs P5-H5 and P7-H7, the left and right side activations were closer in patients at a certain phase of the movement, while in healthy individuals there was a greater difference.

In the lower limb task, the expected motor joints are the joints RK and RA. As shown in Fig.8, there are six matching synergistic structures between healthy individuals and patients. During the task, it can be observed that both healthy participants and patients need to maintain stability and balance by activating the upper limb joints.

The specificity vector pairs show that at a certain phase of the movement, the upper limb is less involved in the patients than in the healthy participants.

E. Analysis of the Involvement of Specific Synergistic Joints

To quantify the degree of involvement of the joints in the synergistic structure during the movement, we analyzed the specific cluster centroid vectors obtained above. We selected the three joints with the highest weight in each specificity vector, generated heat maps and overlaid them to obtain

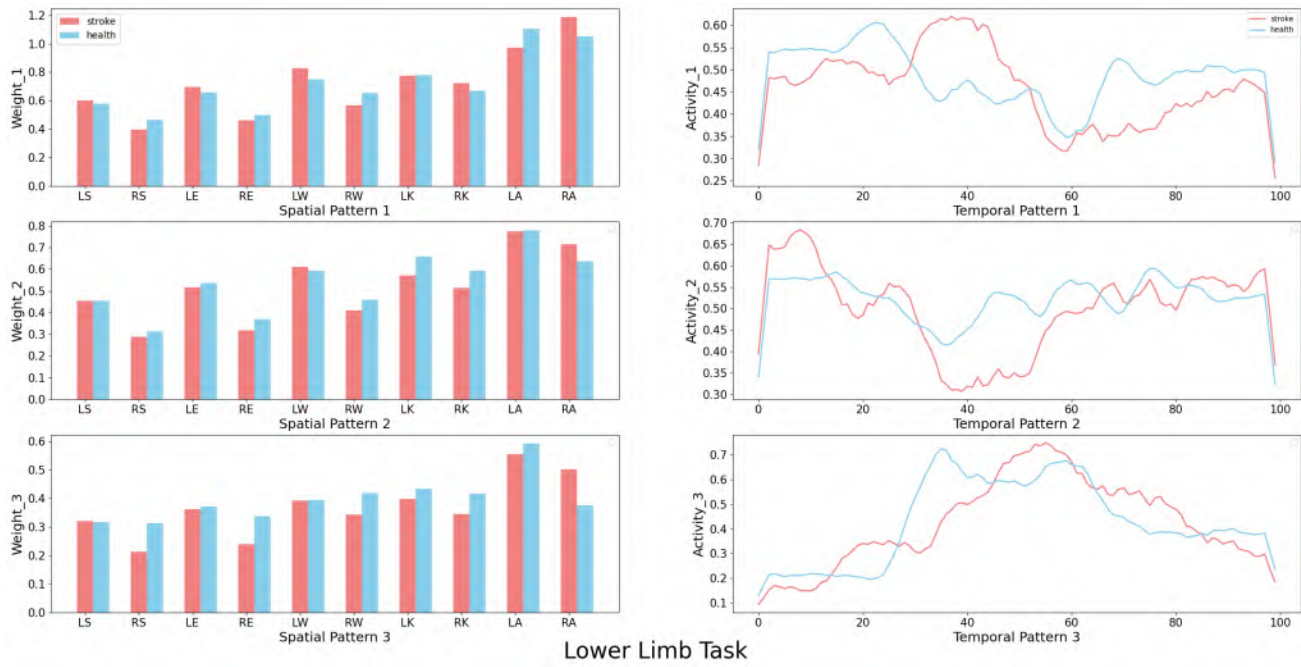


Fig. 6. The spatio-temporal patterns of the lower limb task

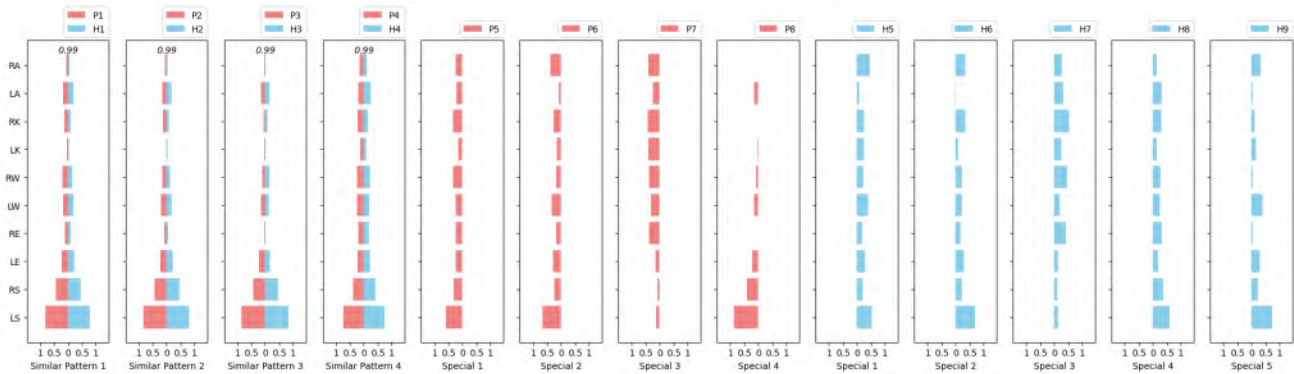


Fig. 7. Matching results of motion synergy vectors for the upper limb task

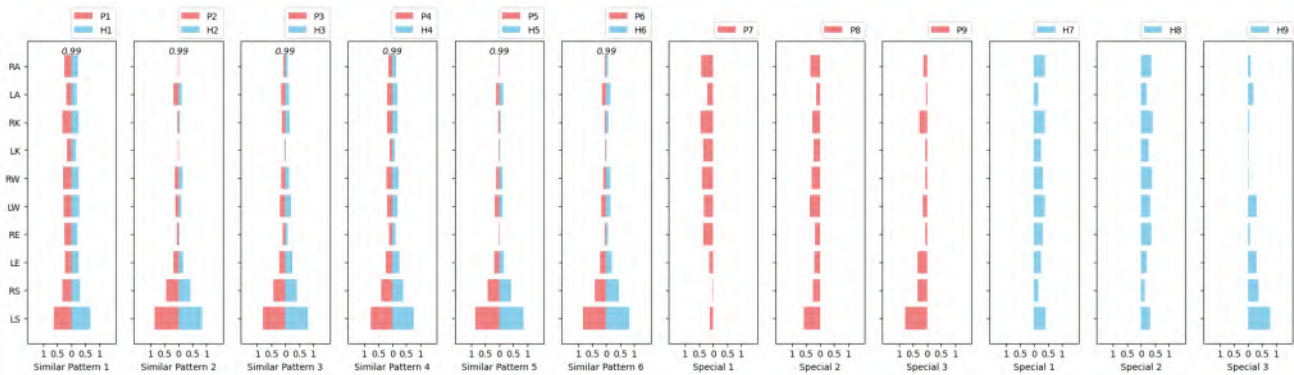


Fig. 8. Matching results of motion synergy vectors for the lower limb task

specific synergistic joint heat maps for healthy participants and patients. As shown in Fig.9.

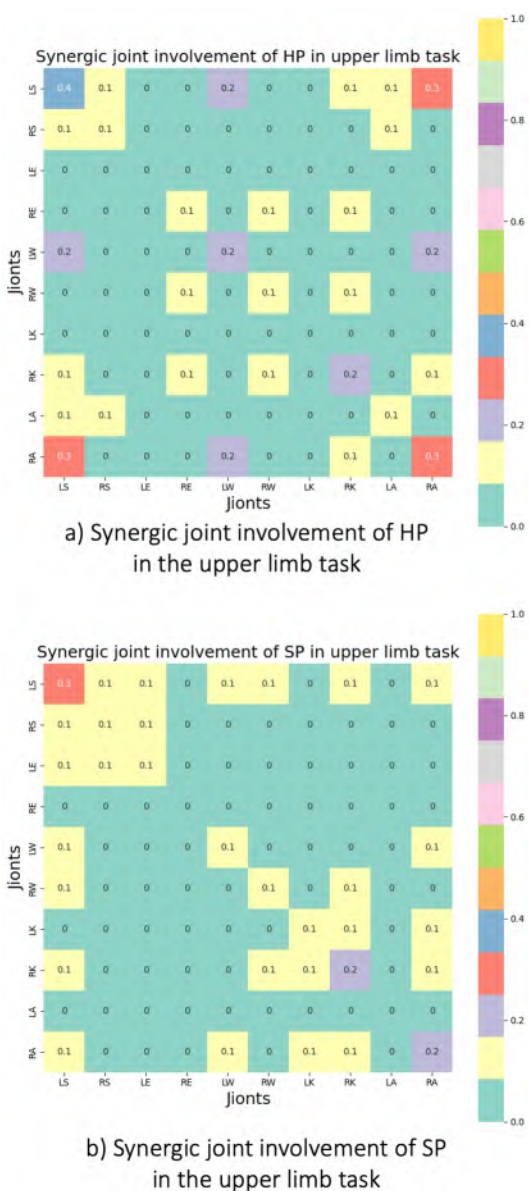


Fig. 9. Heat map of synergistic joint involvement in the upper limb tasks

From Fig.9 a) and b), it can be obtained that in the upper limb movement synergistic structure, the contralateral upper limb joint LE was more involved in the SP group than in the HP group, as well as the contralateral lower limb joint LK. The synergy between the ipsilateral upper limb joints (RW, RE, and RK) was stronger in the HP group than in the SP group. From the above results, it is clear that patients (the SP group) recruited more of the contralateral joints to participate in the movement of the upper limb, while the ipsilateral joint synergy was stronger in the healthy participants (the HP group).

From Fig.10 a) and b) we can find that in the lower limb motor synergistic structure, the contralateral upper limb joint LE was more involved in the SP group than in the

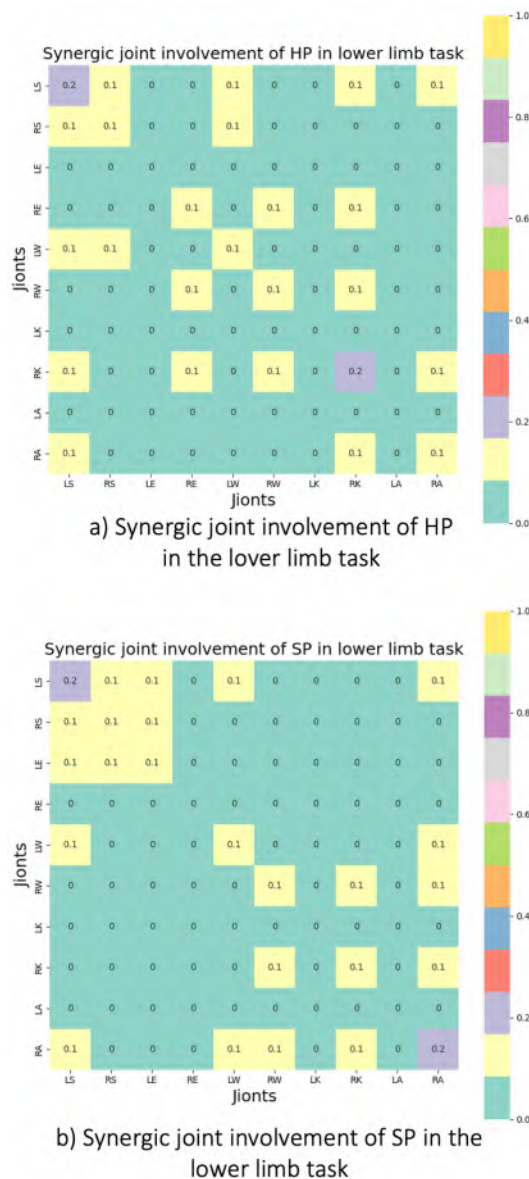


Fig. 10. Heat map of synergistic joint involvement in the lower limb tasks

HP group. The synergy between the ipsilateral joints RE and RK was stronger in the HP group than in the SP group. We hypothesized that the patients' contralateral elbow joint synergy patterns were typically altered during single-leg stance movements. We were excited by this finding and returned to the video for verification. Through the video, we found a particular pattern, every patient had an involuntary bending of the contralateral arm to the body side when the leg was raised, a finding that could provide a new basis for the rehabilitation process.

V. DISCUSSION AND CONCLUSION

From the above results, we observed that during the upper limb movements, the lower limb joints of healthy participants were more involved in synergistic structures. This may be because healthy participants identify the upper limb task

as an easy task that can be completed faster and more relaxed during motion, at which point the lower limb is relied upon to adjust the center of gravity and maintain balance quickly. On the other hand, the task is of greater difficulty for the patients and requires slow and effortful completion to minimize changes in the gravity center.

In all tasks, the patients exhibited altered synkinetic structures in the contralateral elbow joint. In particular, we found a strong coupling between the patients' support leg and the contralateral arm during single-leg stance, which was verified in the patients' video, as detailed in Section IV.

In this study, we present a novel approach to identifying specific patterns of motor synergy induced by disease-altered biomechanics and the central nervous system. It may provide a new method for the assessment of rehabilitation of patients due to ageing, disease and injury, as well as new ideas for further quantitative assessment on the degree of motor rehabilitation. In the future, it may be specifically applied in the analysis of patients' movements to give precise recommendations and scores based on their specific movement patterns. However, there are still some limitations to this study. For instance, there may be different patterns of motor synergy between various types of motor function impairments. Therefore, future work needs to be explored for different types of patients and to increase the sample size.

REFERENCES

- [1] S. Aoi and T. Funato, "Neuromusculoskeletal models based on the muscle synergy hypothesis for the investigation of adaptive motor control in locomotion via sensory-motor coordination," *Neuroscience Research*, vol. 104, pp. 88–95, 2016.
- [2] V. C. K. Cheung, X.-C. Zheng, R. T. H. Cheung, and R. H. M. Chan, "Modulating the structure of motor variability for skill learning through specific muscle synergies in elderlies and young adults," *IEEE Open Journal of Engineering in Medicine and Biology*, vol. 1, pp. 33–40, 2020.
- [3] L. Rinaldi, L.-F. Yeung, P. C.-H. Lam, M. Y. C. Pang, R. K.-Y. Tong, and V. C. K. Cheung, "Adapting to the mechanical properties and active force of an exoskeleton by altering muscle synergies in chronic stroke survivors," *IEEE Transactions on Neural Systems and Rehabilitation Engineering*, vol. 28, no. 10, pp. 2203–2213, 2020.
- [4] K. Zhao, Z. Zhang, H. Wen, B. Liu, J. Li, Andrea d'Avella, and A. Scano, "Muscle synergies for evaluating upper limb in clinical applications: A systematic review," *Heliyon*, vol. 9, no. 5, p. e16202, 2023.
- [5] L. Rinaldi, L.-F. Yeung, P. C.-H. Lam, M. Y. C. Pang, R. K.-Y. Tong, and V. C. K. Cheung, "Adapting to the mechanical properties and active force of an exoskeleton by altering muscle synergies in chronic stroke survivors," *IEEE Transactions on Neural Systems and Rehabilitation Engineering*, vol. 28, no. 10, pp. 2203–2213, 2020.
- [6] A. Falaki, H. J. Jo, M. M. Lewis, B. O'Connell, S. De Jesus, J. McInerney, X. Huang, and M. L. Latash, "Systemic effects of deep brain stimulation on synergic control in parkinson's disease," *Clinical Neurophysiology*, vol. 129, no. 6, pp. 1320–1332, 2018.
- [7] J. H. Hollman, N. G. Buenger, S. G. DeSautel, V. C. Chen, L. R. Koehler, and N. D. Schilaty, "Altered neuromuscular control in the vastus medialis following anterior cruciate ligament injury: A recurrence quantification analysis of electromyogram recruitment," *Clinical Biomechanics*, vol. 100, p. 105798, 2022.
- [8] T. Tani, S. Imai, N. Inoue, N. Kanazawa, and K. Fushimi, "Association between volume of patients undergoing stroke rehabilitation at acute care hospitals and improvement in activities of daily living," *Journal of Stroke and Cerebrovascular Diseases*, vol. 32, no. 2, p. 106872, 2023.
- [9] P. Pattath, E. C. Odom, X. Tong, X. Yin, and S. M. Coleman King, "A comparison of acute ischemic stroke patients discharged to inpatient rehabilitation vs a skilled nursing facility: The paul coveredell national acute stroke program," *Archives of Physical Medicine and Rehabilitation*, vol. 104, no. 4, pp. 605–611, 2023.
- [10] A. G. Geeslin, D. F. Lemos, and M. G. Geeslin, "Knee ligament imaging: Preoperative and postoperative evaluation," *Clinics in Sports Medicine*, vol. 40, no. 4, pp. 657–675, 2021.
- [11] G. C. Fanelli, "Multiple ligament injured knee: Initial assessment and treatment," *Clinics in Sports Medicine*, vol. 38, no. 2, pp. 193–198, 2019.
- [12] A. R. Fugl-Meyer, L. Jääskö, I. A. Leyman, S. Olsson, and S. Steglind, "The post-stroke hemiplegic patient. 1. a method for evaluation of physical performance," *Scandinavian journal of rehabilitation medicine*, vol. 7 1, pp. 13–31, 1975.
- [13] D. Bacciu, S. Chessa, C. Gallicchio, A. Micheli, L. Pedrelli, E. Ferro, L. Fortunati, D. L. Rosa, F. Palumbo, F. Vozzi, and O. Parodi, "A learning system for automatic berg balance scale score estimation," *Engineering Applications of Artificial Intelligence*, vol. 66, pp. 60–74, 2017.
- [14] C. Wang, L. Peng, Z.-G. Hou, Y. Li, Y. Tan, and H. Hao, "A hierarchical architecture for multisymptom assessment of early parkinson's disease via wearable sensors," *IEEE Transactions on Cognitive and Developmental Systems*, vol. 14, no. 4, pp. 1553–1563, 2022.
- [15] C. Wang, L. Peng, Z.-G. Hou, and P. Zhang, "The assessment of upper-limb spasticity based on a multi-layer process using a portable measurement system," *IEEE Transactions on Neural Systems and Rehabilitation Engineering*, vol. 29, pp. 2242–2251, 2021.
- [16] L. Maistrello, D. Rimini, V. C. K. Cheung, G. Pregolato, and A. Turolla, "Muscle synergies and clinical outcome measures describe different factors of upper limb motor function in stroke survivors undergoing rehabilitation in a virtual reality environment," *Sensors*, vol. 21, no. 23, 2021.
- [17] V. Cheung, A. Turolla, M. Agostini, S. Silvoni, C. Bennis, P. Kasi, S. Paganoni, P. Bonato, and E. Bizzi, "Muscle synergy patterns as physiological markers of motor cortical damage," *Proceedings of the National Academy of Sciences of the United States of America*, vol. 109, pp. 14 652–6, 08 2012.
- [18] V. C. K. Cheung, B. M. F. Cheung, J. H. Zhang, Z. Y. S. Chan, S. C. W. Ha, C.-Y. Chen, and R. T. H. Cheung, "Plasticity of muscle synergies through fractionation and merging during development and training of human runners," *Nature Communications*, vol. 11, no. 1, p. 4356, 2020.
- [19] K. Xiang, W. Wang, Z.-G. Hou, C. Zhang, J. Wang, W. Shi, Y. Jiao, and T. Lin, "Muscle synergy analysis based on nmf for lower limb motor function assessment," in *2022 IEEE International Conference on Robotics and Biomimetics (ROBIO)*, 2022, pp. 2116–2121.
- [20] C. Wang, L. Peng, Z.-G. Hou, J. Li, T. Zhang, and J. Zhao, "Quantitative assessment of upper-limb motor function for post-stroke rehabilitation based on motor synergy analysis and multi-modality fusion," *IEEE Transactions on Neural Systems and Rehabilitation Engineering*, vol. 28, no. 4, pp. 943–952, 2020.
- [21] R. Tibshirani, G. Walther, and T. Hastie, "Estimating the Number of Clusters in a Data Set Via the Gap Statistic," *Journal of the Royal Statistical Society Series B: Statistical Methodology*, vol. 63, no. 2, pp. 411–423, 01 2002.